Simulated Gas Turbine Casing Response to Rotor Blade Pressure Excitation

Author:
Forbes, Gareth Llewellyn; Randall, Robert Bond

Publication details:
Proceedings of the Fifth Australasian Congress on Applied Mechanics
pp. 414-419

Event details:
5th Australasian Congress on Applied Mechanics
Brisbane, Australia

Publication Date:
2007

DOI:
https://doi.org/10.26190/unsworks/430

5th Australasian Congress on Applied Mechanics, ACAM 2007
10-12 December 2007, Brisbane, Australia

Simulated Gas Turbine Casing Response to Rotor Blade Pressure Excitation

G.L. Forbes[1] and R.B. Randall[1]

[1]*School of Mechanical and Manufacturing Engineering, University of New South Wales, Australia*

Abstract: Non-intrusive measurement of blade condition within gas turbines is of major interest within all areas of their use. It is proposed that the measurement of the casing vibration, due to the aerodynamic-structural interaction within the turbine, could provide a means of blade condition monitoring and modal parameter estimation. In order to understand the complex relationship between blade vibrations and casing response, an analytical model of the casing and simulated pressure signal associated with the rotor blades is presented. A mathematical formulation is undertaken of the internal pressure signal due to both the rotating bladed disk as well as individual blade vibrations and the solution of the casing response is formulated. Excitation by the stator blades and their contribution to the casing response is also investigated. Some verification of the presented analytical model is provided by comparison with Finite Element Analysis results for various rotor rotational speeds.

Keywords: blade faults, casing vibration, gas turbines, simulation.

1 Introduction

The external non-intrusive measurement of blade condition within a gas turbine is the goal of most online condition monitoring systems for gas turbines. The measurable parameter which is monitored and the sort of correlation between blade condition and changes within this parameter, vary between the different techniques employed; such as power output, blade arrival timing, blade strain gauge measurements and casing vibration amongst others. This study is focused on the latter of these parameters. Understanding of the interaction between the excitation forces and the casing vibration response is therefore sought in order to derive a methodology for monitoring blade condition. This study is the beginning of a continuing program to attempt to extract the blade vibration signals from the overall measured casing vibration.

Only a few authors are known to have previously attempted to find a correlation between casing vibration and blade condition [1, 2]. Mathioudakis et al [1] used an inverse filtering technique to reconstruct the internal pressure signal within a gas turbine from the measured casing vibrations by constructing transfer functions between the two signals. This demonstrated that the statistical properties of measured casing acceleration signals can be linked with engine operation conditions. Hartin et al [2] attempted to construct an analytical model of the casing response under the influence of a rotating pressure signal and then to verify these results with experimental measurements. The conclusions presented, however, were inconclusive as to the ability of the developed model.

Current non-contact blade vibration measurement techniques are being developed *in-house* by engine manufacturers with the dominant method used being the measurement of blade arrival times using proximity probes [3, 4]. Blade tip timing methods use one or multiple sensors located around the turbine casing to measure the arrival of individual blades and then to form correlations between these measurements and the blade vibration parameters. In service blades undergo forced vibrations from some multiple of shaft speed, or from asynchronous sources. Synchronous vibrations are caused by periodic aerodynamic loadings, which are inherent to the periodic internal geometry of gas turbines, synchronous vibrations are measured relatively easily with tip timing methods; however 3-6 probes are usually used [3, 4]. Asynchronous vibrations, such as rotating stall, compressor surge and blade flutter, which usually occurs at a blade natural frequency, are not as easily analysed from proximity probe measurements. The proposed method of measurement of casing vibrations to determine blade vibration characteristics has a discernible advantage over the current tip timing technique, as it does not require perforation of the casing, and possibly only a single measurement point on the casing surface per rotor stage is needed. Indeed, a single measurement point may be sufficient for a number of stages, as accelerometer measurements at a particular stage have been shown to contain frequency information for adjacent stages [1].

2 Formulation of Excitation Forces

The casing of a gas turbine under test conditions can only be excited by two groups of forces [1], viz: a) forces transmitted through casing attachments to the engine and running gear, ie transmission of the turbine and engine component vibrations through their bearing attachments to the casing, b) forces from aerodynamic/casing structure interaction, though both groups of forces should contain the same information due to the reciprocal nature of the excitation. The second group of forces can be broken down into the supposed constituent excitations being; (i) rotating pressure field from the pressure profile around each rotor blade (ii) propagation of acoustic waves inside the casing (iii) pressure fluctuations from turbulent and impulsive flows. Within this study only the forces from (i) are modelled, however forces from (iii) are to be studied in more depth in future work. The interaction between the casing structural motion and fluid pressures is restricted to be non-coupled, ie the motion of the casing has no influence on the pressure distributions.

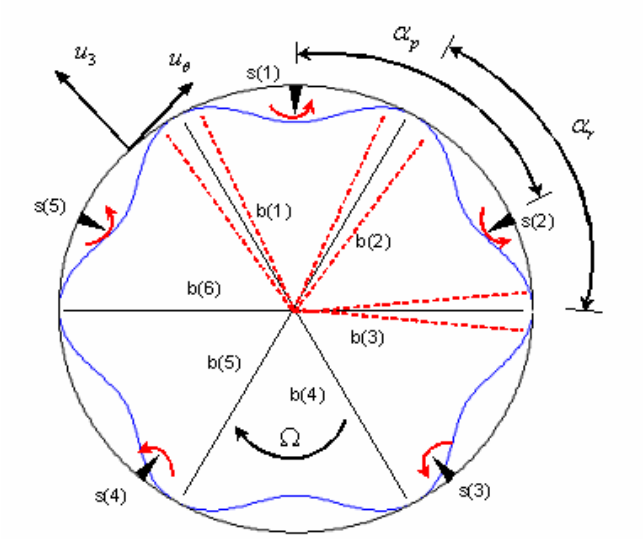

Figure 1 Cross section of gas turbine showing loadings

A cross sectional view of the model which was used in this study can be seen in Figure 1. This consists of an arrangement of '*b*' rotor blades (being 6) and '*s*' stator blades (being 5), the rotating pressure forces and moments due to the stator blades are also shown in Figure 1, and are explained as follows.

Forced vibration of the blades results from the fact that as each rotor blade passes a stator blade, a pressure is built up and drops off in a periodic fashion and causes the blade to oscillate. This force is assumed to be sinusoidal with the blades behaving as a simple oscillator. Therefore, the blade motion will be sinusoidal with an amplitude β and at the frequency of the driving force, this being the stator blade passing frequency ω_{spf} . The static pressure field ,(i), around each blade, which is modelled as a simple sinusoid, then follows the motion of each blade as they rotate around inside the gas turbine at shaft speed. This blade motion causes a phase modulation of the pressure peaks associated with each blade. This is modelled essentially by a Hanning function (one period of a raised sinusoid) that is attached to each blade, and vibrates about its equilibrium position in the rotating reference frame with the characteristics of the blade's forced vibration. The mathematical representation of this rotating pressure force with blade vibration terms is:

$$P_n = P_a + P.e^{jb\left[\theta-\Omega t-\beta\sin\left(\omega_{spf}t+\gamma_r\right)\right]}.\left[H\left(\theta-\Omega t-\alpha_r+\frac{\pi}{b}\right)-H\left(\theta-\Omega t-\alpha_r-\frac{\pi}{b}\right)\right] \quad (1)$$

$$\gamma_r = \frac{2\pi\left(r-1\right)}{b}-\text{round}\left(\frac{s\left(r-1\right)}{b}\right)\frac{2\pi}{s} \quad (2)$$

where H is the Heaviside function and '*r*' is the *r*th rotor blade. γ_r is the phase offset of the force on a rotor blade as it passes any stator blade, with blade (1) passing stator (1) at zero phase.

The excitation forces on the stator blades are equal and opposite to the excitation force exerted on the rotor blade during their relative passage past each other. This force is taken as applying a direct local moment on the casing surface. It is noted that this does not take into account the stator blade vibrations (assumed stiffer than the rotor blades). The mathematical representation of the local moment on the casing surface is given below:

$$T_p = M_0 \sin\left(\omega_{bpf} t + \gamma_p\right) \delta\left(\theta - \alpha_p\right) \left(\frac{1}{R}\right) \tag{3}$$

$$\gamma_p = \text{round}\left(\frac{b\left(p-1\right)}{s}\right)\frac{2\pi}{b} - \frac{2\pi\left(p-1\right)}{s} \tag{4}$$

where '*p*' is the *p*th stator blade, ω_{bpf} is the blade pass frequency and γ_p is the phase offset of the force on a stator blade as it is passed by any rotor blade.

3 Analytical casing response solutions

The casing is modelled analytically as a circular ring, using thin shell theory with free-free boundary conditions for the analytical modelling. The physical properties of the shell are shown in Table 1. Solutions for the rotating pressure loading and the stator blade loading are solved for separately, due to the fact that the rotating pressure wave requires a different set of mode shape functions compared to the spatially stationary local moment loadings which are able to be solved using the normal mode shapes. The results for each solution form are then combined for a total casing response.

Table 1 Geometric and material properties of ring

Density	$\rho = 7.85\times10^{-9}\, Ns^2/mm^4$
Young's Modulus	$E = 20.6\times10^4\, N/mm^2$
Mean Radius	$R = 100mm$
Radial Thickness	$h = 2mm$

Solving first for the stator blade loadings, using modal expansion techniques with the assumed mode shapes being:

$$\begin{aligned} U_{3k} &= \cos n\left(\theta - \phi_p\right) \\ U_{\theta k} &= C_{nk} \sin n\left(\theta - \phi_p\right) \end{aligned} \tag{5}$$

The value of ϕ_p will be such that the mode shape will orientate itself to cause the least resistance to the applied moment giving:

$$\phi_p = -\frac{\pi}{2n} + \alpha_p \tag{6}$$

The solution of the modal participation factor in equation (7), as shown below, will give the time form of the response.

$$\ddot{P}_{nk} + 2\zeta_{nk}\omega_{nk}\dot{P}_{nk} + \omega_{nk}^2 P_{nk} = F_{nk} \tag{7}$$

Solution for a local moment was given by [5], this being done by adding an extra energy term for the displacement that a moment induces in the surface of a shell, and a modified forcing term ensues. The forcing term is shown to be given by:

$$F_{nk} = \frac{1}{\rho h N_{nk}} \int_{\theta} U_{3k} \left[\frac{\partial \left(T_p R \right)}{\partial \theta} \right] d\theta \tag{8}$$

Solution for the local moment is obtained with substitution of the forcing function, equation (3) into equations (7)-(8).

$$u_3 = \sum_{n=1}^{\infty} \sum_{k=1}^{2} \sum_{p=1}^{s} \frac{M_0 n}{\rho h N_{nk}} A_{nk} \left[\sin\left(\omega_{bpf} t + \gamma_p - \phi_{nk} \right) \right] \cos n\left(\theta - \phi_p \right) \tag{9}$$

where M_0, ω_{nk}, A_{nk}, ϕ_{nk} are the applied moment magnitude, ring natural frequency, non-dimensional amplitude and non-dimensional phase of a circular ring for mode '*n,k*'. These later three values are well documented in any vibration reference text, such as [5].

$$N_{nk} = \pi \left(1 + C_{nk}^2 \right) R \tag{10}$$

It can also be approximated [5] that,

$$\begin{aligned} C_{n1} &\approx -1/n \\ C_{n2} &\approx n \end{aligned} \tag{11}$$

Solution for the rotating pressure is undertaken using a method shown in [6]. Additionally, one is directed to [7, 8] which both deal with shells under the loading condition that is variable in both space and time. Under these loading conditions, different mode shape functions as stated below are required:

$$\begin{aligned} U_{3k} &= e^{jn(\theta - \alpha_r)} \\ U_{\theta k} &= C_{nk} j e^{-jn(\theta - \alpha_r)} \end{aligned} \tag{12}$$

Using the modified mode shapes in equation (12) and also substituting the resonance frequency for a moving load on a circular ring of $\tilde{\omega}_{nk} = \omega_{nk} / n$ [7, 8], into the modal participation factor equation with the utilisation of the solution for the generalised force vector as in [6], gives:

$$F_{nk} = \frac{1}{2\rho h N_{nk}} \int_{\theta} P_n conj\left(U_{3k} \right) R d\theta \tag{13}$$

A complete solution for the radial displacement can then be shown to be:

$$u_3 = \mathrm{Re}\left[\sum_{n=1}^{\infty} \sum_{k=1}^{2} \sum_{v=0}^{\infty} \sum_{r=1}^{b} a_{nk} e^{j\left[n\Omega t - v\left(\omega_{spf} t + \gamma_r \right) \right]} e^{-j\psi_1} e^{jn(\theta - \alpha_r)} + b_{nk} e^{j\left[n\Omega t - v\left(\omega_{spf} t + \gamma_r \right) \right]} e^{-j\psi_2} e^{jn(\theta - \alpha_r)} \right] \tag{14}$$

where $J_v\left(b.\beta \right)$ is the Bessel function of the first kind, and:

$$a_{nk} = \frac{P.R.f\left(n \right).J_v\left(b.\beta \right)}{2\rho h N_{nk} \sqrt{\left(n^2 \tilde{\omega}_{nk}^2 - n^2 \left(\Omega - v\omega_{spf} / n \right)^2 \right)^2 + 4\zeta^2 \tilde{\omega}_{nk}^2 n^4 \left(\Omega - v\omega_{spf} / n \right)^2}} \tag{15}$$

$$f\left(n \right) = \begin{cases} \dfrac{2}{b-n} \sin\left(\dfrac{\left(b-n \right)\pi}{b} \right) & n \neq b \\ \dfrac{2\pi}{b} & n = b \end{cases} \tag{16}$$

$$\psi_1 = \tan^{-1}\left(\frac{2\zeta\left(\frac{\Omega - \nu\omega_{spf}/n}{\tilde{\omega}_{nk}}\right)}{1-\left(\frac{\Omega - \nu\omega_{spf}/n}{\tilde{\omega}_{nk}}\right)^2}\right) \tag{17}$$

Similarly the b_{nk} and ψ_2 terms can be found.

4 Results

Results were obtained for the radial displacement of a circular ring, under the simulated forces acting on it as defined earlier, using the analytical equations of (9) and (14), as well as from a finite element model. An arbitrary value of a natural frequency of the blades was chosen to be 500Hz, the displacement was then analysed over a range of 75-125Hz for the shaft speed Ω, such that this blade natural frequency was traversed. Both the analytical and finite element model used light structural damping in the shell. The maximum amplitude of deflection for any rotor blade was limited to $\pi/2b$, or one quarter of the distance between the adjacent blades, and this therefore limits β to a small enough value such that only up to ± 3 sidebands were needed in the analytical analysis.

Inspection of equations (9) and (14) gives rise to the form of the response observed for the analytical model in Figure 2 and Figure 3. it is seen that the stator blade loadings will cause a response at the blade passing frequency, and the displacement due to the pressure loadings surrounding each blade will also give a component at the blade passing frequency as well as an infinite set of sidebands around the blade passing frequency spaced by multiples of shaft speed and the stator passing frequency, which are due to the motion of the blades under forced vibration. For an input shaft speed of 80Hz in Figure 2 the blade pass frequency of 480Hz is indicated by a double arrow, and the modulation side bands at multiples of stator blade passing frequency, 400Hz, are indicated by the single arrows. A waterfall plot over the surface of the frequencies for a range of shaft speeds can be seen in Figure 3. The magnitude of the sidebands at stator passing frequencies can be seen to be dominant, and they also peak as the blade natural frequency is traversed, at 100Hz. The peak in the first(positive) stator pass frequency side band is the most prominent, and is indicated in both graphs in Figure 3. It is these sidebands which contain the information corresponding to blade vibrations.

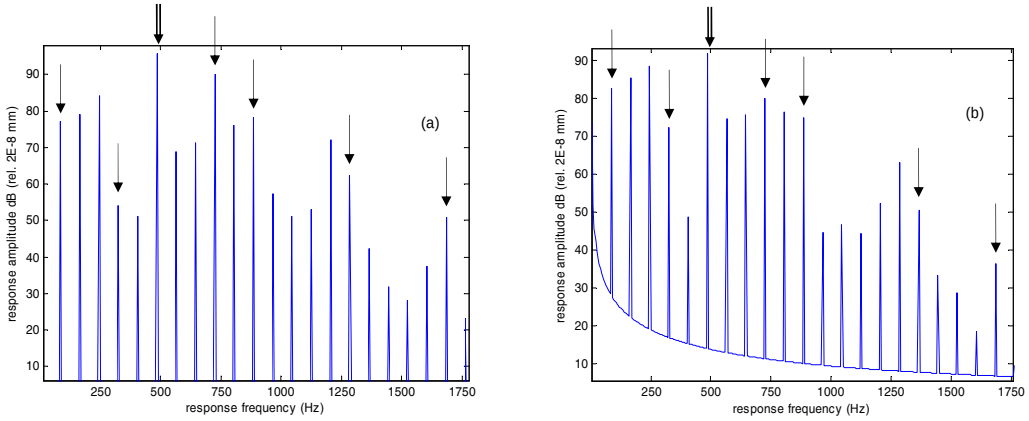

Figure 2 Radial casing response at shaft speed of 80Hz, (a) analytical, (b) finite element

The corresponding results obtained from a finite element model under the same loading conditions are shown alongside the results for the analytical modelling in Figure 2 and Figure 3. The results from the finite element model correlate well with the analytical results, however some differences may be noted in the response magnitude. This is believed to have arisen from the soft spring supports and the finite axial length of this model. The amount of effort and modelling subtleties required to model such loading conditions within a finite element package is not adequately conveyed by the small mention it gets within this work; however, the model was constructed as follows. The casing was modelled as a cylindrical shell with 50 elements around its circumference, and one element along its axial length.

Soft spring supports with damping were added at the stator blade locations of s(1) and s(3), refer to Figure 1. The spatial and time varying loads were applied and solved with a transient dynamic solution technique in the commercial FEA package ANSYS using a technique similar to that outlined by [9], using the HHT integration algorithm with numerical damping. When the initial load was applied on the FEA model some spurious transients were observed due to these initial conditions, the results were taken after these transients had died away. Some residual effect of the very low frequency suspension resonances is still seen however.

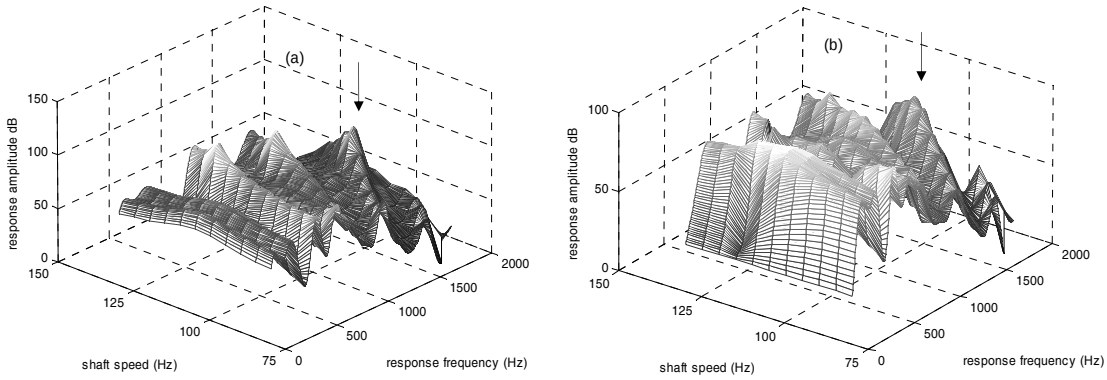

Figure 3 Casing response at shaft speeds from 75-125Hz, (a) analytical, (b) finite element

5 Conclusion

An analytical and finite element model of a gas turbine undergoing simulated operating conditions has been developed to predict the casing's vibration response under these loadings. Comparison of these models shows a good correlation between the two, with the important feature of the results being that the response has peaks when a blade natural frequency is traversed. The aim of this project was to determine how blade vibrations would influence vibration measurements on the casing surface, and the results showed that response of the casing contains information about forced blade vibrations inside the casing such that external non-intrusive measurements of these vibrations could allow for blade vibration monitoring. This gives the basis of an alternative technique to the current industry standard of measuring blade vibrations through blade arrival times, using proximity probes which require perforation of the casing.

References

[1] Mathioudakis, K., E. Loukis, and K.D. Papailiou. *Casing vibration and gas turbine operating conditions*. 1989. Toronto, Ont, Can: Publ by American Soc of Mechanical Engineers (ASME), New York, NY, USA.

[2] Hartin, J.R. and E. Quandt, *Forced response of a cylindrical shell due to a rotating harmonic internal pressure loading.* Active Control of Vibration and Noise, ASME, 1994. **DE. 75**: p. 337-342.

[3] Heath, S., *A New Technique for Identifying Synchronous Resonances Using Tip-Timing.* Journal of Engineering for Gas Turbines and Power, 2000. **122**(2): p. 219-225.

[4] Zielinski, M. and G. Ziller, *Noncontact Blade Vibration Measurement System for Aero Engine Application.* American Institute of Aeronautics and Astronautics, 2005(ISABE).

[5] Soedel, W., *Vibrations of shells and plates*. 2nd ed. 1993, New York: Marcel Dekker. xix, 470 p.

[6] Forbes, G.L. and R.B. Randall, *Resonance Phenomena of an Elastic Ring under a Moving Load.* Journal of Sound and Vibration, 2007. **Submitted**.

[7] Huang, S.C. and W. Soedel, Effects of Coriolis Acceleration on the Free and Forced in-plne Vibrations of Rotating Rings on Elastic Foundation.. Journal of Sound and Vibration, 1987. **115**(2): p. 253-274.

[8] Huang, S.C. and W. Soedel, *Response of rotating rings to harmonic and periodic loading and comparison with the inverted problem.* Journal of Sound and Vibration, 1987. **118**(2): p. 253-270.

[9] Wu, J.-J., A.R. Whittaker, and M.P. Cartmell, *Use of finite element techniques for calculating the dynamic response of structures to moving loads.* Computers and Structures, 2000. **78**(6): p. 789-799.